Magnetic structure of the two-dimensional XY antiferromagnet $Sr_2CoSi_2O_7$ studied using single-crystal neutron diffraction

Rajesh Dutta [1,2,*] Henrik Thoma [1,2,†] Andrew Sazonov,[3] Bálint Náfrádi,[4] Martin Meven [1,2] Arsen Gukasov [5]
Vilmos Kocsis,[6,7] Uli Zeitler,[8] Alessandro Puri,[8,9] Yusuke Tokunaga,[6,10] Yasujiro Taguchi,[6] Yoshinori Tokura,[6,11,12]
Sándor Bordács,[13] István Kézsmárki,[14] and Vladimir Hutanu [1,2,‡]

[1]*Institut für Kristallographie, RWTH Aachen Universität, 52066 Aachen, Germany*
[2]*Jülich Centre for Neutron Science at Heinz Maier-Leibnitz Zentrum, 85747 Garching, Germany*
[3]*European Spallation Source ERIC, P.O. Box 176, SE-221 00 Lund, Sweden*
[4]*EPFL, Laboratory of Nanostructures and Novel Electronic Materials, 1015 Lausanne, Switzerland*
[5]*Laboratoire Léon Brillouin, CEA-CNRS, CE-Saclay, 91191 Gif-sur-Yvette, France*
[6]*RIKEN Center for Emergent Matter Science (CEMS), Wako, Saitama 351-0198, Japan*
[7]*Institut für Festkörperforschung, Leibniz IFW Dresden, 01069 Dresden, Germany*
[8]*High Field Magnet Laboratory (HFML-EMFL), Radboud University, Toernooiveld 7, 6525 ED Nijmegen, The Netherlands*
[9]*CNR-IOM-OGG c/o ESRF-The European Synchrotron, 71 Avenue des Martyrs, 38000 Grenoble, France*
[10]*Department of Advanced Materials Science, University of Tokyo, Kashiwa 277-8561, Japan*
[11]*Quantum-Phase Electronics Center, Department of Applied Physics, University of Tokyo, Tokyo 113-8656, Japan*
[12]*Department of Applied Physics, University of Tokyo, Hongo, Tokyo 113-8656, Japan*
[13]*Department of Physics, Institute of Physics, Budapest University of Technology and Economics,
Müegyetem rkp. 3., H-1111 Budapest, Hungary*
[14]*Department of Experimental Physics V, University of Augsburg, 86159 Augsburg, Germany*

We report a combined polarized and unpolarized neutron diffraction study on a multiferroic $Sr_2CoSi_2O_7$ (SCSO) single crystal below and above the antiferromagnetic ordering temperature $T_N = 6.5$ K. Unpolarized neutron diffraction measurements at 15 K confirm the melilite-type tetragonal $P\bar{4}2_1m$ space group as the parent structure of SCSO. The low temperature study at 2.3 K, in contrast, reveals symmetry lowering with the orthorhombic $Cmm'2'$ and $P2_12_1'2'$ magnetic space groups being equally possible. In these $Cmm'2'$ and $P2_12_1'2'$ magnetic space groups we obtain a very similar ordered magnetic moment about 2.86 and 2.94 μ_B/Co^{2+}, respectively, which lies in the ab plane. Our spin polarized flipping ratio measurements under an applied magnetic field of 6 T in the paramagnetic state support the results of our bulk magnetization data, indicating strong easy-plane spin anisotropy, responsible for the in-plane order below T_N.

I. INTRODUCTION

Melilite-type multiferroic $A_2MB_2O_7$ (A = Ca, Sr, Ba; M = Co, Mn, Cu, Fe; and B = Ge, Si) compounds are interesting potential candidates for studying exotic low-dimensional quantum phenomena including magnetic, electronic and structural correlations along with the magnetoelectric effect [1–5]. These materials belong to quasi-two-dimensional (2D) square lattice Heisenberg antiferromagnets (SLHAF) with spin $S \geqslant 1/2$ [6,7] and have been intensively studied to explore their multiferroic properties and exotic magnetic behavior [8–13]. For the magnetic ground state, the important ingredients of these materials are the strong easy-plane spin anisotropy and the Dzyaloshinskii-Moriya interaction (DMI). These two interactions, combined with the large A cations separating the magnetic M layers, play a crucial role in realizing

the quasi 2D nature with a nonvanishing weak out-of-plane interaction [13]. On the other hand, the microscopic structure is also a key feature for the observed magneto-electric (ME) effects as they are driven by the spin dependent d-p hybridization mechanism between the transition metal 3d and the ligand 2p orbitals [2,8].

The most intensively studied compounds in this family are the germanates $Ba_2MGe_2O_7$ (M = Co, Mn, Cu). They mainly differ from each other by their spin microstructure, formed by different magnetic exchange interactions. In $Ba_2MnGe_2O_7$, the interplane exchange coupling is antiferromagnetic ($J > 0$) doubling the magnetic unit cell along the c axis, whereas it is ferromagnetic ($J < 0$) in $Ba_2CoGe_2O_7$ with strong easy-plane single ion anistropy (SIA). In case of $Ba_2CuGe_2O_7$, DMI is stronger than SIA resulting in a spiral magnetic structure. In the last few decades, the true symmetry of the nuclear and magnetic structure of multiferroic germanates has been studied via single crystal neutron and synchrotron X-ray diffraction [1,14–18].

In addition to the sensitivity of the character of the magnetic ground state to the choice of the transition metal ion,

*Corresponding author: rajesh.dutta@frm2.tum.de

†Corresponding author: henrik.thoma@frm2.tum.de

‡Present address: FRM II, Technische Universität München, 85747 Garching, Germany; vladimir.hutanu@frm2.tum.de
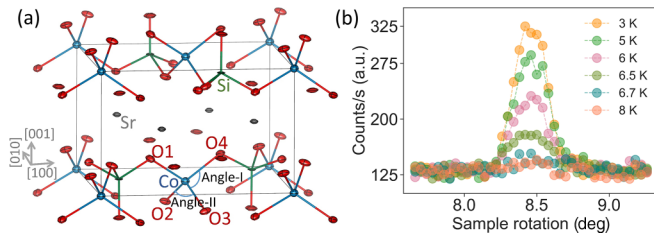
FIG. 1. (a) Illustration of the refined nuclear structure of the SCSO single crystal at 15 K in the $P\bar{4}2_1m$ space group. Ellipses represent the anisotropic displacement parameters. Oxygen are named to denote angle and bond distance which are given in Table III. (b) Temperature dependent sample rotation scans performed on (300) magnetic reflection using neutron diffraction.

TABLE I. Single crystal neutron diffraction experiment & refinement details.

space group	tetra. $P\bar{4}2_1m$	ortho. $P2'_12_12'$	ortho. $Cm'm2'$
T (K)	15	2.3	2.3
a, c (Å)	8.105, 5.228	8.091, 5.213	11.412, 5.211
$(\sin\theta/\lambda)_{max}$ (Å^{-1})	0.84	0.84	0.84
measured reflections	2176	2081	2081
refinement reflections	907	1661	986
R_{int}	2.8%	2.7%	2.3%
refinement on	F	F	F
R_F, wR_F	2.76%, 5.41%	2.78%, 6.76%	2.45%, 5.93%
GOF	3.76	2.05	2.04
Weight	$1/\sigma^2(F_o)$	$1/\sigma^2(F_o)$	$1/\sigma^2(F_o)$
extinction corrections	isotropic	isotropic	isotropic
type	Gaussian type 1	Gaussian type 1	Gaussian type 1
extinction coefficient	0.94	0.29	0.29

the magnetic and ME properties can also be tuned substituting the nonmagnetic sites. Thus, it is interesting to study how the substitution of Ge by Si affects the ME properties and the adopted magnetic structure in this compound family. Compared to germanates, silicate family members (Ba, Sr, Ca)$_2$CoSi$_2$O$_7$ are not well explored except few of them which show quite complex magnetic structure completely different from germanates. For example, Ba$_2$CoSi$_2$O$_7$ shows a quasi-one-dimensional monoclinic $C2/c$ structure with magnetic wave vector (1/2, 1/2, 1/2) [19]. In case of Ca$_2$CoSi$_2$O$_7$, the low temperature magnetic structure was described within orthorhombic $P2_12'_12'$ with magnetic wave vector (1/3, 1/3, 1) [20], but there is no report on the refined magnetic structure of Sr$_2$CoSi$_2$O$_7$ (SCSO) below T_N. In the lack of the low-temperature structural information, the paramagnetic $P\bar{4}2_1m$ symmetry, as depicted in Fig. 1(a), was assumed in former studies to describe the physical properties. This severe lack of information on both the nuclear and magnetic structure of SCSO at low temperature makes a more detailed microscopic study of SCSO indispensable.

Moreover, it is crucial to investigate the detailed structural changes with temperature for a further justification whether the structure is correlated with the microscopic physical phenomena like the spin-dependent *d-p* hybridization mechanism, and the induced local electric field in the CoO$_4$ tetrahedron and its distortion under temperature. Therefore, in this article, we have taken a significant step towards the understanding of the magnetic structure using single crystal neutron diffraction at 2.3 K. Additionally, we have carried out spin polarized flipping ratio (FR) measurements using polarized neutron diffraction to understand the magnetic spin anisotropy in the paramagnetic phase.

II. EXPERIMENTAL METHODS AND DATA TREATMENT

Single crystal neutron diffraction measurements on SCSO grown by the floating zone method [21,22] were carried out on hot-neutron four-circle diffractometer (HEiDi) [23] at the FRM II reactor, Heinz Maier-Leibnitz Zentrum (MLZ), Germany. The measurements were performed using a wavelength $\lambda = 0.793$ Å obtained from a Ge(422) vertical focusing monochromator using an Er filter to suppress $\lambda/2$ contamination. For low-temperature experiments, a closed-cycle He cryostat was mounted in the Eulerian cradle of the diffrac-

tometer. Temperature dependent intensities of the selected magnetic and nuclear Bragg reflections were measured in the range of 11 to 3 K during the cooling process. For the structure determination, complete data sets were collected at 15 and 2.3 K. The data reduction to generate the hkl list in a SHELX format was performed using PRON2K10 [24] program. The nuclear and magnetic structure refinements were carried out using the JANA2006 software [25]. The refinement details are given in Table I.

For the microscopic study of the field induced magnetic structure in the paramagnetic phase, polarized neutron flipping ratios were measured at 10 K in SCSO on the Very Intense Polarized (VIP) diffractometer [26] equipped with large position sensitive detector (PSD) at the Orphée reactor at the Laboratoire Léon Brillouin (LLB) in Saclay, France. The FR experiment was carried out in an applied external magnetic field of 6 T and with a neutron wavelength of 0.84. For the measurements, the SCSO single crystal was oriented with the [551] and [115] direction almost parallel to the vertical axis of the instrument and thus to the field direction. For the magnetic moment refinement using the MAG2POL software [27], weak Bragg reflections with a measurement accuracy I/dI < 50, corresponding to an intensity below around 2% of the maximal observed value, were excluded due to their high uncertainty in the calculated asymmetry. As the FR measurements are performed in the paramagnetic phase, all the moments are assumed to point in the field direction and thus, only an induced ferromagnetic (FM) component with zero antiferromagnetic (AFM) contribution is considered in the refinement.

Additional macroscopic high field magnetization measurements on a SCSO single crystal were performed using a vibrating sample magnetometer at the high field magnet laboratory, Radboud University, The Netherlands.

III. RESULTS AND DISCUSSION

Figure 1(b) shows a few selected sample rotation scans performed on the purely magnetic reflection (300) using unpolarized neutron diffraction on the SCSO single crystal. It confirms the onset of the magnetic ordering is to be at
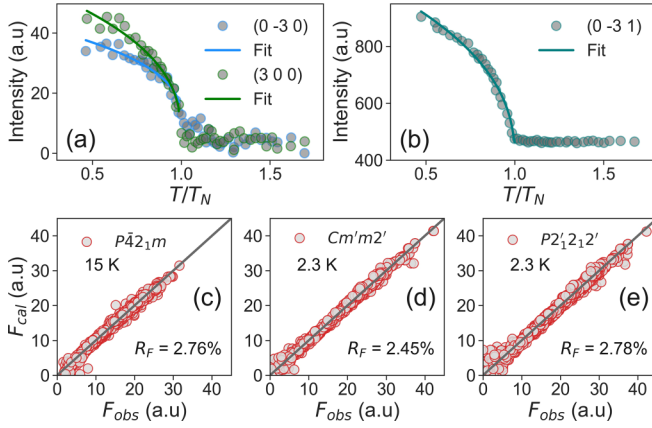
FIG. 2. (a), (b) Integrated intensities of reflections of purely magnetic origin (left) and both magnetic and nuclear origin (right) as function of temperature. Error bars are inside the symbols. Solid lines represents the fit to Eq. (1). The corresponding fitted critical exponents are denoted in the figure. (c)–(e) Observed and calculated structure factors are presented for both SSG representations along with corresponding reliability factors R_F.

around 6.5 K. Temperature evolution of the integrated intensities of the chosen mixed (nuclear plus magnetic) $(0\bar{3}1)$, and pure magnetic (300), $(0\bar{5}0)$ Bragg reflections are presented in Figs. 2(a) and 2(b). The intensities of both type of reflections decrease with increasing temperature up to $T_N = 6.5$ K. Above T_N, the intensities are near to zero for the magnetic reflections, whereas that for the mixed reflections remain finite and constant, representing the somewhat temperature independent nuclear contribution. We have fitted the integrated intensity (I) of the magnetic peaks up to T_N using a power law behavior given as

$$I = I_n + I_0[(T_N - T)/T_N]^{2\beta}, \tag{1}$$

where I_n is the nuclear intensity, I_0 is the magnetic intensity at $T = 0$ K, and β is the critical exponent. From the fit we have obtained $\beta = 0.20 \pm 0.08$ close to the value for 2D-XY spin systems similar to BCGO [1].

For determining the low temperature magnetic structure of SCSO, we first need precise information on the nuclear structural parameters. For that purpose, we have carried out a structural refinement of our neutron diffraction data at 15 K using the typical melilite crystal structural model with space group $P\bar{4}2_1m$. The starting model parameters were taken from the isostructural compound BCGO [15]. All symmetry unrestricted atomic positions were refined together with atomic displacement parameters, scale factor, and the extinction parameters. The obtained final structure is displayed in Fig. 1. Figure 2(c) shows the good agreement between the observed and calculated structure factors validating the assumed tetragonal $P\bar{4}2_1m$ space group as the nuclear structure model for SCSO. The refined parameters, such as atomic positions and atomic displacements, are given in Table II.

For the low temperature magnetic phase at 2.3 K, we have carried out in a first step the magnetic Rietveld least-square refinement with a nuclear structure model fixed to the results of the 15 K data discussed above. After a proper convergence of the magnetic parameters was achieved, we released in a second step additional to the atomic positions and displacement parameters to refine the magnetic and nuclear structure simultaneously. No significant differences were found in the atomic positions between these 15 and 2 K data (see Table II). For the refinement model, magnetic representation analysis suggests two possible magnetic Shubnikov space groups (SSG) with a lower symmetry than the parent structure. These are orthorhombic $Cm'm2'$ with axes (1,-1,0|1, 1, 0|0,0,1) and $P2_1'2_12'$ with axes (0,-1,0|-1,0,0|,0,0,-1). Both SSG allow a canting of the AFM moment leading to finite magnetization within the ab plane, with a uniform order along the c axis, like in its sister compound BCGO [1,15]. As the magnetic symmetry breaks the fourfold inversion axis of the parent structure, tetragonal magnetic domains are expected for the AFM moments. In zero magnetic field, an equal population of all four domains is expected for both SSG making them indistinguishable from a refinement point of view. Thus, the refinements for both SSG result in similar structural and magnetic parameters, which are presented in Table II. Figure 3 shows the magnetic structure in $P2_1'2_12'$ setting indicated by

TABLE II. Refined fractional atomic coordinates (x, y, z) and isotropic atomic displacement parameters U_{iso} (Å^2) of SCSO for different space groups from the single crystal neutron diffraction data at 2.3 and 15 K.

ion	$P\bar{4}2_1m$ (15 K)				$P2_1'2_12'$ (2.3 K)				$Cm'm2'$ (2.3 K)			
	x	y	z	U_{iso}	x	y	z	U_{iso}	x	y	z	U_{iso}
Sr1	0.66543(7)	0.16543(5)	0.50699(3)	0.00214(6)	0.66531(4)	0.16581(8)	0.506529(5)	0.00309(5)	0.66538(4)	0.50000(5)	−0.50294(3)	0.00344(7)
Sr2									0.00000	0.66554(6)	0.51067(5)	0.00321(5)
Co	0.00000	0.00000	0.00000	0.00290(12)	0.00000	0.00000	0.00000	0.00309(9)	0.25000	0.25000	0.00000	0.00394(7)
Si1	0.36181(1)	0.13818(9)	0.05521(5)	0.00191(2)	0.36148(4)	0.13812(8)	0.05499(8)	0.00391(7)	0.13850(8)	0.50000	0.04793(9)	0.00396(2)
Si2									0.50000	0.36179(2)	−0.06173(5)	0.00346(6)
O1-1	0.19166(7)	0.07964(2)	0.20126(7)	0.00346(5)	−0.19259(6)	−0.07828(9)	−0.20540(4)	0.00361(3)	0.19170(6)	0.38422(7)	0.20032(7)	0.00363(5)
O1-2					0.08057(2)	−0.19062(4)	0.19693(8)	0.00385(11)	0.38673(3)	0.30366(7)	−0.20208(8)	0.00346(7)
O2-1	0.36025(2)	0.13974(8)	0.74474(3)	0.00423(7)	0.36421(7)	0.14337(4)	0.74461(5)	0.00391(7)	0.13991(4)	0.50000	0.74387(2)	0.00305(6)
O2-2									0.50000	0.36062(6)	0.74569(4)	0.00322(7)
O3-1	0.50000	0.00000	0.16419(4)	0.00303(3)	0.50000	0.00000	0.16298(6)	0.00391(7)	0.00000	0.50000	0.16269(7)	0.00344(7)
O3-2									0.50000	0.50000	0.16334(7)	0.00385(9)
μ_B^{AFM}						2.941(5)					2.860(4)	

FIG. 5. Refined free AFM component and R_F against fixed FM component. The dashed vertical line shows the value obtained from the free model. Rectangle box guides the deviation window for R_F.

is why we have fixed the FM component to $\approx 0.02 \mu_B/$Co according to magnetization data and refined only the AFM component which is about $2.94 \mu_B/$Co in P centering and $2.86 \mu_B/$Co for C centering. Right hand side of Fig. 5 displays the refinement quality (R_F) and free AFM moment against the fixed FM component from 0.01 to $1.6 \mu_B/$Co. The free AFM component decreases gradually with decreasing the fixed FM component. Even if the standard uncertainty of the FM component is very small, fixing the FM component does not improve the R_F significantly, it stays almost unchanged ($\leqslant 0.1\%$). This can indicate that the standard uncertainties based on linearized least square methods should not be used as the only criterion. Therefore, the structure presented in Fig. 3 is a constrained model with a fixed FM moment to be $\approx 0.02 \mu_B/$Co.

From the unpolarized neutron diffraction at zero magnetic field, it seems difficult to distinguish between these two described SSG. Other transport and physical property measurements might be helpful to decide the actual symmetry of the structure at low temperature. A similar scenario appeared in case of the BCGO compound [15] but the electric polarization measurements excluded the possibility of $P2_1'2_12'$ SSG as this SSG does not allow the spontaneous electric polarization at zero magnetic field. In the $Sr_2CoSi_2O_7$ compound we do not have this possibility to validate the statement as it seems to not induce the spontaneous electric polarization at zero magnetic field [32]. Also, we have refined the magnetic structure at 2.3 K keeping its nuclear structure the same as in the PM phase. The refined parameters are given in Table IV along with its reliability factor and it indicates that the considerations of low temperature magnetic structure in tetragonal parent nuclear unit cell ($P\bar{4}2_1m$) is quite reasonable.

Figure 4(b) shows the high field bulk magnetization data of SCSO obtained at 2 K under the field applied up to 32 T along the different crystallographic directions. In the linear region we can obtain the anisotropy in the magnetic susceptibility (χ) which is about $\chi_{[110]}/\chi_{[001]} \approx 2$, similar to the value obtained in the BCGO sample [1].

Polarized neutron flipping-ratio (FR) measurements in SCSO were performed above T_N in the paramagnetic state at 10 K and in external magnetic fields of 6 T. This technique is suitable for studying FM and paramagnetic materials since classical FR technique gives a polarization independent scattering cross section in the collinear AFM materials due to the presence of magnetic 180° domains. The FR ratio $R(Q)$ of each Bragg reflection of scattering vector Q can be expressed

FIG. 3. Refined magnetic structure of SCSO at 2.3 K projected in the *ab* plane with the magnetic propagation vector $\mathbf{q}_m = (000)$. Gray and dashed black squares correspond to the orthorhombic $P2_1'2_12'$ and $Cm'm2'$ unit cell, respectively. The slight canting of the magnetic moments (blue arrows) is discussed in the text.

thick gray unit cell while for $Cm'm2'$ setting unit cell is rotated 45° and indicated by dashed black unit cell. The characteristic parameter $\mathcal{K}$, which is an angle between the diagonal and the $O-Co-O$ bond made of upper two oxygen atoms in CoO_4 tetrahedron, and indicated in Fig. 3 reflects basically the rotation of CoO_4 tetrahedron between neighbored sites and is an important parameter in the analysis of the induced electric polarization [2]. We have tabulated $\mathcal{K}$ and other structural parameters of the CoO_4 tetrahedron, like the dihedral angle ($\mathcal{D}$), bond distance and other angles in Table III to draw a comparison with other melilites.

In both SSG when both components of the magnetic moment of Co^{2+} are released during the refinement, it shows a big canting angle with a large FM component ($0.9 \pm 0.06 \mu_B/$Co) which does not match well with the bulk magnetization data. Our low-field magnetization data displayed in Fig. 4(a) shows a tiny FM component of $\approx 0.02 \mu_B/$Co at 2 K similar to the values reported elsewhere [28,29]. However, the refined AFM moment of $2.9 \pm 0.04 \mu_B/$Co is slightly lower than the saturation moment of $\approx 3.5 \mu_B/$Co. Such amount of AFM moment of Co^{2+} was also found in BCGO [1]. This
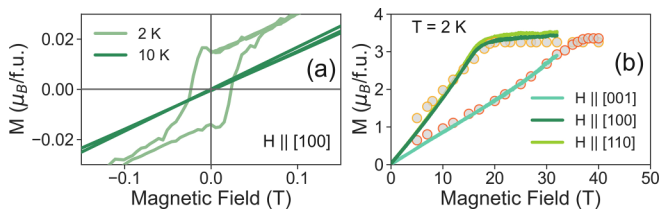

FIG. 4. (a) Low-field and (b) high-field bulk magnetization curve of SCSO obtained at various temperatures. Solid lines represent the experimental data. Solid circles (right) are calculated magnetic moments along [001] and [100] in pink and orange color, respectively, using linear spin wave theory.
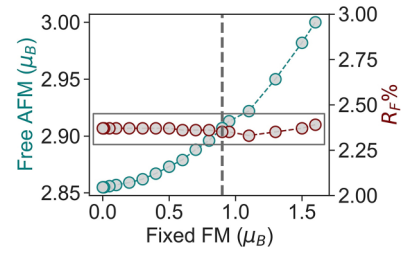
TABLE III. Comparison between the angles and bond distances inside the MO_4 (M = Co, Mn) tetrahedra. Angle-I and angle-II are marked in Fig. 1.

SSG	angle-I(^{o})	angle-II(^{o})	O1−Co(Å)	O2−Co(Å)	$\mathcal{K}$(^{o})	$\mathcal{D}$(^{o})
			$Sr_2CoSi_2O_7$			
$P\bar{4}2_1m$ (15 K)	106.33 (4)	115.95 (4)	1.984 (10)	1.984 (10)	23.26 (4)	77.27 (7)
$P2_1'2_12'$ (2 K)	105.78 (8)	114.98 (8)	1.968 (2)	1.998 (2)	22.16 (3)	77.13 (3)
$Cm'm2'$ (2 K)	107.79 (7)	115.64 (6)	1.978 (2)	1.986 (2)	21.59 (4)	77.15 (2)
			$Ba_2CoSi_2O_7$			
$P\bar{4}2_1m$ (293 K) [30]				1.964 (4)		
$C2/c$ (293 K) [31]			1.978 (4)	1.963 (4)		
			$Ba_2CoGe_2O_7$ [15]			
$P\bar{4}2_1m$ (10.4 K)	106.04	116.56	1.969	1.969	21.80	77.95
$P\bar{4}2_1m$ (2.2 K)	106.09	116.46	1.970	1.970	21.79	77.84
$Cmm2$ (2.2 K)	106.14	116.61	1.969	1.971	21.91	77.86
			$Ba_2MnGe_2O_7$ [17]			
$P\bar{4}2_1m$ (110 K)	106.1 (2)	116.43 (3)	2.042 (6)	2.042 (6)	21.91 (3)	77.80 (4)

as

$$R(Q) = I^+/I^- \tag{2}$$

and

$$I^\pm(Q) \propto F_N^2 + F_{M\perp}^2 + P^\pm \cdot (F_N^* F_{M\perp} + F_N F_{M\perp}^*), \tag{3}$$

where I^+ and I^- are the diffracted intensities with spins parallel (+) and antiparallel (−) to the applied magnetic field which are measured with the polarization vector (P) of the incident neutron beam. F_N and F_M are the nuclear and magnetic structure factors, respectively. However, another quantity instead of R, so called asymmetry has been used to present the data and it is given by

$$A = (I^+ - I^-)/(I^+ + I^-). \tag{4}$$

We have carried out a restricted magnetic moment refinement, which denotes that all the moments are assumed to point in the field direction in paramagnetic phase. As a result, the refinement provides only the field-induced FM moment of the Co atom along that direction. Figure 6 displays the refined asymmetry values for both data sets with magnetic field along the [551] and [115] directions and overall fit qualities (χ_r^2). The obtained magnetic moment along the [551] and [115] directions is 0.61(2) and 0.39(8) μ_B/Co, respectively. The induced FM moment along [551] is lower than the expected

TABLE IV. Refined fractional atomic coordinates (x, y, z) and isotropic atomic displacement parameters U_{iso} (Å^2) of SCSO keeping the nuclear structure in $P\bar{4}2_1m$ symmetry.

	$P\bar{4}2_1m$ (2.3 K), R_F = 3.1%, and GOF = 3.14			
ion	x	y	z	U_{iso}
Sr1	0.66540(4)	0.16540(8)	0.50650(4)	0.00238(6)
Co	0.00000	0.00000	0.00000	0.00333(12)
Si1	0.36172(10)	0.13827(2)	0.05464(3)	0.00333(3)
O1	0.19157(2)	0.07936 (6)	0.20115(7)	0.00346(7)
O2	0.36032(9)	0.13967(2)	0.74474(4)	0.00423(7)
O3	0.50000	0.00000	0.16285(4)	0.00303(2)

value of $\approx 1\mu_B$/Co along [110] at 10 K and 6 T [33]. This could be due to the fact that the applied field direction [551] which is not exactly the same as the [110] direction and the moment becomes smaller when the field rotates from [110] towards [001] due to the anisotropy. Nevertheless, our bulk magnetization and FR measurements reflect the magnetic anisotropic character nicely, between the ab plane and c axis of the crystal. This could in principle reflect the similar value of magnetic single-ion anisotropy in both compounds SCSO and BCGO.

In addition, we have calculated the magnetization near the high field regime using linear spin wave theory (LSWT) using the SPINW package [34]. In principle, the total length of the Co spin ($S = 3/2$) was given in the calculation and then normalized with the reduction of saturation moment value from the experimental values [32]. Here we assume a spin only moment without consideration of spin-orbit coupling. The spin Hamiltonian used for this calculation is given by

$$\mathcal{H} = J \sum_{i,j} \left(S_i^x S_j^x + S_i^y S_j^y + \Delta S_i^z S_j^z) \right] + \Lambda \sum_i \left(S_i^z \right)^2$$
$$- \sum_i g\mu_B H^{ex} \cdot \mathbf{S}_i, \tag{5}$$

where J and Δ represent the anisotropic in-plane exchange interactions, Λ represents easy-plane type single ion anisotropy (SIA). H^{ex} is the applied external magnetic field. The computed magnetization curves are plotted on the experimental
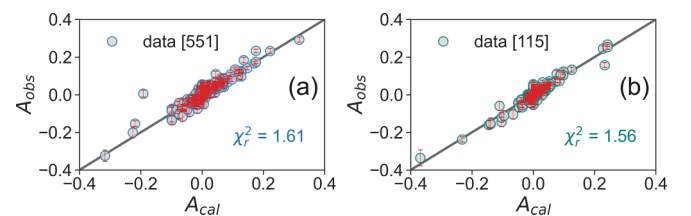
FIG. 6. Calculated and observed asymmetry (A) is plotted for data measured with field applied along [551] (a) and along [115] (b). The corresponding refinement quality is denoted in the figure.

data in the right side of Fig. 4. It is noted that the Co magnetization curve in both SCSO and BCGO compounds behave in the same way, especially as the difference of the saturation field between the *ab* plane and *c* axis magnetization is, for both compounds, about 20 T. However, in the case of $Sr_2CoSi_2O_7$ this difference is only about 4 T, and the ratio of the magnetic susceptibility $\chi_{[110]}/\chi_{[001]} \approx 1.2$ indicates a clearly lower value of the single-ion anisotropy in case of $Sr_2CoGe_2O_7$ [35]. Therefore, it is safe to take the exchange and SIA parameters obtained from the inelastic neutron scattering study on BCGO [13]. The calculation nicely reproduces the experimental data in the high field region above 7 T, and most importantly, it accounts the onset of the saturation moment found in Ref. [32]. In our calculation we started with the SIA optimization as it plays an important role in the saturation region of the magnetization curve along the *c* axis while it tries to compensate the Zeeman term at high field. In this way, we found a slightly higher value for the SIA than in BCGO with about $\Lambda = 1.3$ meV close to a field of 15 T and 0.6 meV at the saturation field of ≈ 36 T. For the in-plane magnetization, this SIA response is almost silent as the spins are already in the plane but slight anisotropic *g* values ($g_{x=y} = 2.15$ and $g_z = 2.05$) were introduced while the exchange interactions ($J = 0.19$, $\Delta \approx 1.16$) were being adjusted. In order to reproduce the low field magnetization data one needs the information on good values and scheme of DMI and the *g* tensor, while introducing spin-orbit coupling might improve as long as its before further Zeeman-term splitting. However, a mean-field approximation approach could be the better choice for macroscopic measurements; nevertheless, LSWT could account the macroscopic picture once the actual spin Hamiltonian parameters are available.

IV. CONCLUSION

In summary, we have presented a detailed unpolarized neutron diffraction study on the magnetic structure of a SCSO single crystal at 2.3 and 15 K combined with polarized neutron diffraction FR measurements in its paramagnetic phase and bulk magnetization measurements. From unpolarized neutron diffraction measurements, it is impossible to determine the true symmetry unambiguously, at least from refinement quality. From the restricted refinement model the canted angle we have obtained is to be very small ($<0.4^o$) in the *ab* plane. The measured temperature dependence of the order parameter reveals the 2D-XY type spin character similar as in the qusi-2D BCGO [1,13]. Our FR measurements at 6 T show that the magnetic anisotropy between the *ab* plane *c* axis and are in compatible with bulk magnetization data. Surprisingly, SCSO does not align with its sister compounds like $Ba_2CoSi_2O_7$ and $Ca_2CoSi_2O_7$ rather the magnetic structure and the refined structural parameters of SCSO are very close to the values found in BCGO.

[1] V. Hutanu, A. P. Sazonov, M. Meven, G. Roth, A. Gukasov, H. Murakawa, Y. Tokura, D. Szaller, S. Bordács, I. Kézsmárki, V. K. Guduru, L. C. J. M. Peters, U. Zeitler, J. Romhányi, and B. Náfrádi, Evolution of two-dimensional antiferromagnetism with temperature and magnetic field in multiferroic $Ba_2CoGe_2O_7$, Phys. Rev. B **89**, 064403 (2014).

[2] H. Murakawa, Y. Onose, S. Miyahara, N. Furukawa, and Y. Tokura, Ferroelectricity Induced by Spin-Dependent Metal-Ligand Hybridization in $Ba_2CoGe_2O_7$, Phys. Rev. Lett. **105**, 137202 (2010).

[3] M. Soda, M. Matsumoto, M. Månsson, S. Ohira-Kawamura, K. Nakajima, R. Shiina, and T. Masuda, Spin-Nematic Interaction in the Multiferroic Compound $Ba_2CoGe_2O_7$, Phys. Rev. Lett. **112**, 127205 (2014).

[4] K. Penc, J. Romhányi, T. Rõõm, U. Nagel, A. Antal, T. Fehér, A. Jánossy, H. Engelkamp, H. Murakawa, Y. Tokura, D. Szaller, S. Bordács, and I. Kézsmárki, Spin-Stretching Modes in Anisotropic Magnets: Spin-Wave Excitations in the Multiferroic $Ba_2CoGe_2O_7$, Phys. Rev. Lett. **108**, 257203 (2012).

[5] T.-H. Jang, S.-H. Do, M. Lee, H. Wu, C. M. Brown, A. D. Christianson, S.-W. Cheong, and J.-H. Park, Physical properties of the quasi-two-dimensional square lattice antiferromagnet $Ba_2FeSi_2O_7$, Phys. Rev. B **104**, 214434 (2021).

[6] Z. Weihong, R. H. McKenzie, and R. R. P. Singh, Phase diagram for a class of spin-$\frac{1}{2}$ heisenberg models interpolating between the square-lattice, the triangular-lattice, and the linear-chain limits, Phys. Rev. B **59**, 14367 (1999).

[7] S. Chakravarty, B. I. Halperin, and D. R. Nelson, Two-dimensional quantum heisenberg antiferromagnet at low temperatures, Phys. Rev. B **39**, 2344 (1989).

[8] H. Murakawa, Y. Onose, S. Miyahara, N. Furukawa, and Y. Tokura, Comprehensive study of the ferroelectricity induced by the spin-dependent *d-p* hybridization mechanism in $Ba_2XGe_2O_7$ (X = Mn, Co, and Cu), Phys. Rev. B **85**, 174106 (2012).

[9] M. Soda, S. Hayashida, B. Roessli, M. Månsson, J. S. White, M. Matsumoto, R. Shiina, and T. Masuda, Continuous control of local magnetic moment by applied electric field in multiferroics $Ba_2CoGe_2O_7$, Phys. Rev. B **94**, 094418 (2016).

[10] M. Soda, L.-. J. Chang, M. Matsumoto, V. O. Garlea, B. Roessli, J. S. White, H. Kawano-Furukawa, and T. Masuda, Polarization analysis of magnetic excitation in multiferroic $Ba_2CoGe_2O_7$, Phys. Rev. B **97**, 214437 (2018).

[11] A. Zheludev, T. Sato, T. Masuda, K. Uchinokura, G. Shirane, and B. Roessli, Spin waves and the origin of commensurate magnetism in $Ba_2CoGe_2O_7$, Phys. Rev. B **68**, 024428 (2003).

[12] S. Bordács, I. Kézsmárki, D. Szaller, L. Demkó, N. Kida, H. Murakawa, Y. Onose, R. Shimano, T. Rõõm, U. Nagel, S.

Miyahara, N. Furukawa, and Y. Tokura, Chirality of matter shows up via spin excitations, Nat. Phys. **8**, 734 (2012).

[13] R. Dutta, H. Thoma, I. Radelytskyi, A. Schneidewind, V. Kocsis, Y. Tokunaga, Y. Taguchi, Y. Tokura, and V. Hutanu, Spin dynamics study and experimental realization of tunable single-ion anisotropy in multiferroic $Ba_2CoGe_2O_7$ under external magnetic fields, Phys. Rev. B **104**, L020403 (2021).

[14] V. Hutanu, A. Sazonov, H. Murakawa, Y. Tokura, B. Náfrádi, and D. Chernyshov, Symmetry and structure of multiferroic $Ba_2CoGe_2O_7$, Phys. Rev. B **84**, 212101 (2011).

[15] V. Hutanu, A. Sazonov, M. Meven, H. Murakawa, Y. Tokura, S. Bordács, I. Kézsmárki, and B. Náfrádi, Determination of the magnetic order and the crystal symmetry in the multiferroic ground state of $Ba_2CoGe_2O_7$, Phys. Rev. B **86**, 104401 (2012).

[16] A. Sazonov, V. Hutanu, M. Meven, G. Roth, R. Georgii, T. Masuda, and B. Náfrádi, Crystal structure of magnetoelectric $Ba_2MnGe_2O_7$ at room and low temperatures by neutron diffraction, Inorg. Chem. **57**, 5089 (2018).

[17] R. Dutta, H. Thoma, D. Chernyshov, B. Náfrádi, T. Masuda, A. Kriele, and V. Hutanu, Topological analysis of the experimental electron density in multiferroic antiferromagnet $Ba_2MnGe_2O_7$, IEEE Trans. Magn. **58**, 1 (2022).

[18] H. Thoma, V. Hutanu, R. Dutta, A. Gukasov, V. Kocsis, Y. Tokunaga, Y. Taguchi, Y. Tokura, I. Kézsmárki, G. Roth, and M. Angst, Magnetic order and sign of the dzyaloshinskii-moriya interaction in 2-d antiferromagnet $Ba_2CoGe_2O_7$ under applied magnetic field, IEEE Trans. Magn. **58**, 1 (2022).

[19] M. Soda, T. Hong, M. Avdeev, H. Yoshizawa, T. Masuda, and H. Kawano-Furukawa, Neutron scattering study of the quasi-one-dimensional antiferromagnet $Ba_2CoSi_2O_7$, Phys. Rev. B **100**, 144410 (2019).

[20] A. Sazonov, V. Hutanu, M. Meven, G. Roth, H. Murakawa, Y. Tokura, V. K. Guduru, L. C. J. M. Peters, U. Zeitler, L. F. Kiss, D. Szaller, B. Náfrádi, and I. Kézsmárki, Magnetic structure of the magnetoelectric material $Ca_2CoSi_2O_7$, Phys. Rev. B **95**, 174431 (2017).

[21] I. Kézsmárki, D. Szaller, S. Bordács, V. Kocsis, Y. Tokunaga, Y. Taguchi, H. Murakawa, Y. Tokura, H. Engelkamp, T. Rõõm, and U. Nagel, One-way transparency of four-coloured spin-wave excitations in multiferroic materials, Nat. Commun. **5** 3203 (2014).

[22] J. Viirok, U. Nagel, T. Rõ om, D. G. Farkas, P. Balla, D. Szaller, V. Kocsis, Y. Tokunaga, Y. Taguchi, Y. Tokura, B. Bernáth, D. L. Kamenskyi, I. Kézsmárki, S. Bordács, and K. Penc, Directional

dichroism in the paramagnetic state of multiferroics: A case study of infrared light absorption in $Sr_2CoSi_2O_7$ at high temperatures, Phys. Rev. B **99**, 014410 (2019).

[23] M. Meven and A. Sazonov, Heidi: Single crystal diffractometer at hot source, J. large-scale research facilities **1**, A7 (2015).

[24] Program for data reduction of dif4. Version of the Institut fur Kristallographie, RWTH Aachen,

[25] V. Petříček, M. Dušek, and L. Palatinus, Crystallographic computing system JANA2006: General features, Zeitschrift für Kristallographie - Crystalline Materials **229**, 345 (2014).

[26] A. Gukasov, S. Rodrigues, J.-L. Meuriot, T. Robillard, A. Sazonov, B. Gillon, A. Laverdunt, F. Prunes, and F. Coneggo, Very Intense Polarized (VIP) Neutron Diffractometer at the ORPHEE Reactor in Saclay, Phys. Procedia **42**, 150 (2013).

[27] N. Qureshi, *Mag2Pol*: a program for the analysis of spherical neutron polarimetry, flipping ratio and integrated intensity data, J. Appl. Crystallogr. **52**, 175 (2019).

[28] M. Akaki, T. Tadokoro, H. Kuwahara, T. Kihara, and M. Tokunaga, Anisotropic magnetic properties in kermanite $Sr_2MSi_2O_7$ (M = Co, Mn) crystals, J. Korean Phys. Soc. **62**, 1812 (2013).

[29] M. Akaki, J. Tozawa, D. Akahoshi, and H. Kuwahara, Magnetic and dielectric properties of $A_2CoSi_2O_7$ (A = Ca, Sr, Ba) crystals, J. Phys.: Conf. Ser. **150**, 042001 (2009).

[30] B. El Bali and P. Y. Zavalij, Tetragonal form of barium cobalt disilicate, $Ba_2CoSi_2O_7$, Acta Crystallogr., Sect. E **59**, i59 (2003).

[31] R. D. Adams, C. Payen, and T. Datta, Syntheses, structural analyses, and unusual magnetic properties of $Ba_2CoSi_2O_7$ and $BaCo_2Si_2O_7$, Inorg. Chem. **35**, 3492 (1996).

[32] M. Akaki, H. Iwamoto, T. Kihara, M. Tokunaga, and H. Kuwahara, Multiferroic properties of an åkermanite $Sr_2CoSi_2O_7$ single crystal in high magnetic fields, Phys. Rev. B **86**, 060413 (2012).

[33] M. Akaki, T. Tadokoro, T. Kihara, M. Tokunaga, and H. Kuwahara, High magnetic field dependence of magnetodielectric properties in $Sr_2CoSi_2O_7$ crystal, J. Low Temp. Phys. **170**, 291 (2013).

[34] S. Toth and B. Lake, Linear spin wave theory for single-q incommensurate magnetic structures, J. Phys.: Condens. Matter **27**, 166002 (2015).

[35] M. Akaki, D. Yoshizawa, A. Okutani, T. Kida, J. Romhányi, K. Penc, and M. Hagiwara, Direct observation of spin-quadrupolar excitations in $Sr_2CoGe_2O_7$ by high-field electron spin resonance, Phys. Rev. B **96**, 214406 (2017).